Preparation and characterization of ethylene-vinyl acetate nanocomposites: enhanced flame retardant

Manuel Oliveira* and Ana Vera Machado

Abstract

Ethylene-vinyl acetate (EVA) nanocomposites with enhanced flame retardance were prepared by the sol-gel process in the melt. Two EVAs with different vinyl acetate (VA) contents and aluminium isopropoxide were used as organic and inorganic phases. The nanocomposites were prepared in a batch mixer under constant processing conditions and were analysed by several characterization techniques. Aluminium isopropoxide presented low activation energy, which allows the synthesis of the nanoparticles without a post step treatment. The reaction mechanism is proposed. Nanocomposites with smaller and well dispersed metal nanoparticles were produced with an EVA with higher VA content. EVA nanocomposites achieve the requirements for 94 V-0 classification.

Keywords: poly(ethylene vinyl acetate); aluminium nanoparticles; sol-gel reaction; crosslinking

INTRODUCTION

In the last few decades organic-inorganic materials have attracted considerable attention both from academia and industry since they combine the properties of organic and inorganic components. A small amount of well dispersed inorganic filler can improve material properties significantly, such as gas permeability, thermal stability, flame retardance, mechanical performance or chemical resistance. [1–3]

Although a lot of research has been done concerning nanocomposite preparation, the homogeneous dispersion of nanofillers in a polymeric matrix is still a difficult task. The main drawbacks resulting from filler incorporation in a polymeric matrix are particle agglomeration and void formation at the interface of the particles and polymer matrix. [4] Aiming to improve this, the research for new methods led to the use of sol-gel reactions to synthesize inorganic fillers in a polymeric matrix. [5,6] The sol-gel method is based on a hydrolysis-condensation reaction of a metal alkoxide, which allows the synthesis of nanoparticles well dispersed in the polymer matrix. Metal alkoxides are the precursors

most widely used [7] as they can react rapidly with water to form hydroxyl compounds which, in turn, allow fast reactions. [8]

Using the sol-gel method to synthesize hybrid nanocomposites, two different types of materials can be obtained, one containing only weak bonds between the two phases, without motion restriction of the matrix molecules, and the other with covalent bonds between the polymer and metal, which were formed during the hydrolysis-condensation reaction of the metal alkoxide. In the latter, the dispersion of the inorganic nanoparticles increases due to network formation. Therefore the molecular motion of the polymer is restricted and the material properties are improved. [6,9]

Preparation of nanocomposites of ethylene-vinyl acetate (EVA) with the addition of inorganic compounds such as clays or metal hydroxides is a common practice, well described in the literature. [10] For applications such as wire and cables fillers are frequently added
to improve fire retardance and thermal stability, [11] among them aluminium trihydrate. Therefore in this work we aimed to prepare EVA nanocomposites containing aluminium species by a sol-gel reaction in the molten state without the presence of solvent and to investigate the effect of the metal bonded to the EVA backbone on the nanocomposite properties.

Nanocomposites of two EVAs (different vinyl acetate (VA) content and viscosity) and aluminium isopropoxide were prepared in a batch mixer under constant processing conditions. The prepared materials were characterized by rheology, Fourier transform infrared (FTIR) spectroscopy, TGA, crosslinking density measurement, SEM, transmission electron microscopy (TEM) and energy dispersive spectrometry (EDS).

MATERIALS AND METHODS

Materials and reagents

EVA with 12wt% (EVA12, Escorene Ultra UL 00112, melting temperature 96°C) and 27wt%(EVA27, Escorene Ultra UL 00328, melting temperature 71°C) of VA, were supplied by Exxon Mobil (Laramie, USA). Aluminium isopropoxide (Al(Pr-i-O)3), used as received in the powder state, was supplied by Sigma Aldrich (Sintra, Portugal).

Synthesis

The aluminium alkoxide concentration was defined as 25%(w/w), which corresponds to a ratio between VA number and aluminium

alkoxide of 0.36 and 0.81 for EVA12 and EVA27, respectively. The EVA containing aluminium nanoparticles was produced in the melt, in a Haake batch mixer (Rheocord 90; volume 60 cm^3), equipped with two rotors running in a counter-rotating way. The rotor speed was 50 rpm and the set temperature was 90°C (melt temperature around 100°C). The following procedure was implemented to produce the nanocomposites. First pellets of EVA were introduced into the hot mixer; after 3 min the aluminium precursor was added. The sol-gel reaction proceeded for 10 min and the total sample was removed. The

hybrid polymer nanocomposite synthesized with EVA12 was called HPNEVA12 and that synthesized with EVA27 was HPNEVA27.

Characterization

Rheological properties

The rheological behaviour of the initial polymers and prepared materials was determined by oscillatory rheological measurements using a Paar Physica MCR300 rheometer at 90°C. The gap and diameter of the plates were 1 mm and 25 mm , respectively. A nitrogen atmosphere was used to prevent thermo-oxidative degradation. A frequency sweep from 0.1 to 100 Hz under constant strain in the linear viscoelastic region was performed for each sample.

Crosslinking density

The crosslinking density was assessed from the volume swelling degree determined at equilibrium. Around 300 mg of samples were placed in hot xylene at 140°C for 30 h until swelling equilibrium was reached. Then the polymer volume fraction at swelling equilibrium, v_r, was calculated as follows:

$$v_r = \frac{1}{1 + (m_1/m_2)(\rho_2/\rho_1)} \tag{1}$$

where m_1 and m_2 are, respectively, the weight of the swelled sample and the weight of the dried sample and ρ_1 and ρ_2 are, respectively, the polymer and solvent densities (gcm^{-3}).

The Flory-Rehner model was used to determine the crosslinking density. This model coupled with the phantom network assumption gives a correlation between the swelling results and the number of elastic strands, v :

$$v = -\frac{\ln(1 - v_r) + v_r + \chi v_r^2}{v\left(v_r^{1/3} - 0.5 v_r\right)} \tag{2}$$

Where χ is the polymer-solvent interaction parameter, V he molar volume of solvent and v_r is the polymer volume fraction at swelling equilibrium. The polymer-solvent interaction parameter χ was calculated as follows:

$$\chi = \frac{V(\delta_1 - \delta_2)^2}{RT + 0.34} \tag{3}$$

where δ_1 and δ_2 are the solubility parameters of polymer and solvent, respectively, V is the molar volume, R is the universal gas constant and T is the absolute temperature.

FTIR spectroscopy

Infrared spectra were recorded in transmission mode between 400 and 4000 cm^{-1} using a Perkin Elmer 1610, with 32 scans and a resolution of 4 cm^{-1}. Films with thickness around 70μ m were previously prepared by compression moulding in a hot press at 90°C.

Activation energy

The activation energy (E_a) of the HPNEVA27 hybrid was determined using gel content values. The nanocomposite was prepared at three different temperatures (90,100 and 110°C) according to the procedure described above and samples were collected after 3,7 and 10 min of mixing. For all samples, the gel content was measured according to the method described previously. For each temperature, the crosslinking rate was determined as the slope of the gel content versus reaction time, as described by Shieh et al. [12] Then, E_a was calculated from the plot of the crosslinking reaction rate at the three different temperatures as a function of the reciprocal absolute temperature, according to the Arrhenius equation

$$\ln\ k = \ln\ A - \frac{E_a}{R}\frac{1}{T} \tag{4}$$

where k is the crosslinking rate, E_a is the activation energy, R is the gas constant and T is the absolute temperature.

SEM and EDS

SEM analysis was performed with a Leica Cambridge S360 microscope in backscatter mode. The samples were previously fractured in liquid nitrogen and coated with a gold thin film. X-ray microanalysis mapping was performed over 300μ m^2, in the same place where the SEM analysis was done, with an energy dispersive X-ray spectrometer from Link eXL II, Oxford Instruments, attached to the scanning electron microscope.

TEM

Samples of 70 nm thickness were cut using a diamond knife, in a Leica ultramicrotome at −60°C. The cut sections were transferred onto copper grids and then analysed without stain in a Philips CM120 transmission electron microscope.

Thermal stability

The thermal stability of the EVA hybrids was assessed by TGA carried out in a TA Q500 thermobalance. Samples were heated from 30°C to 600°C at 10°Cmin^{-1} under a nitrogen flow (50 mL min^{-1}).

UL94 test

The flammability behaviour of EVA and EVA nanocomposites was investigated according to the UL-94 test using two sets of five

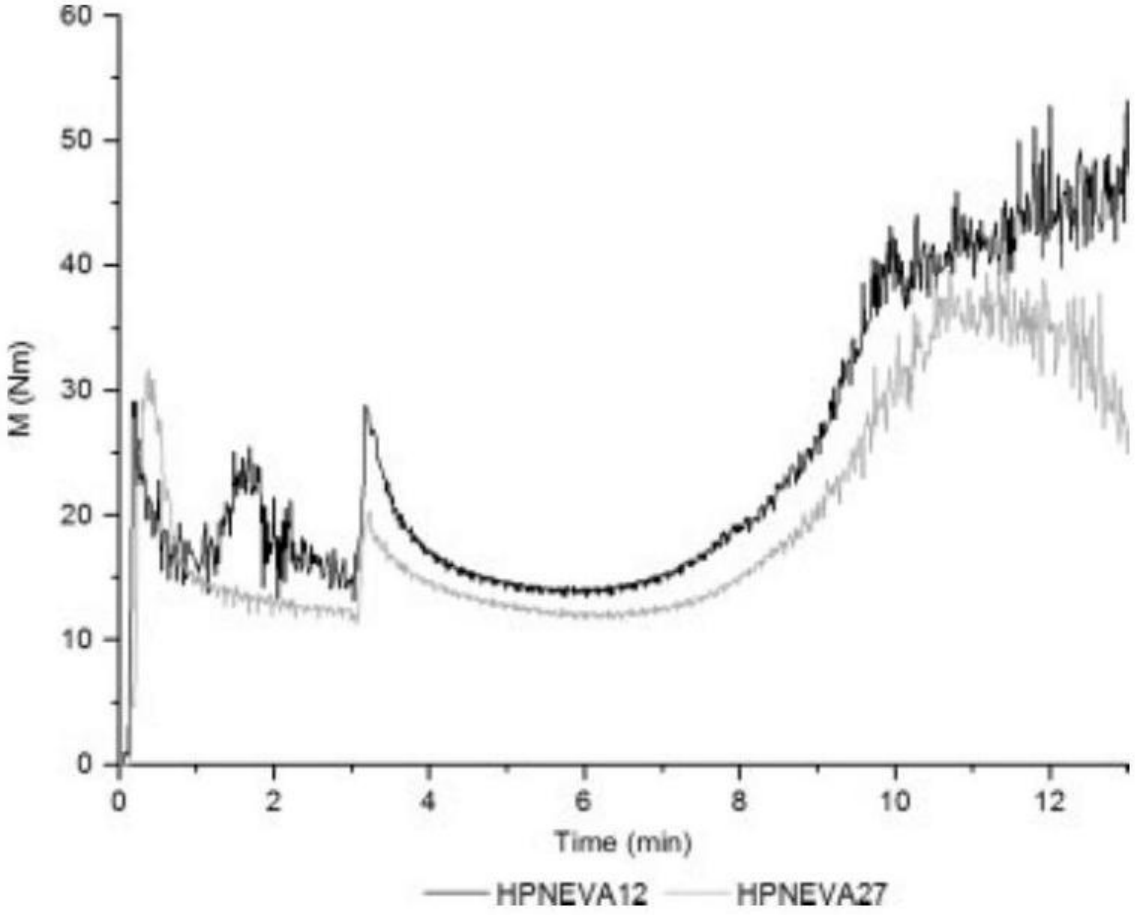

Figure 1. Torque evolution during HPNEVA12 and HPNEVA27 preparation.

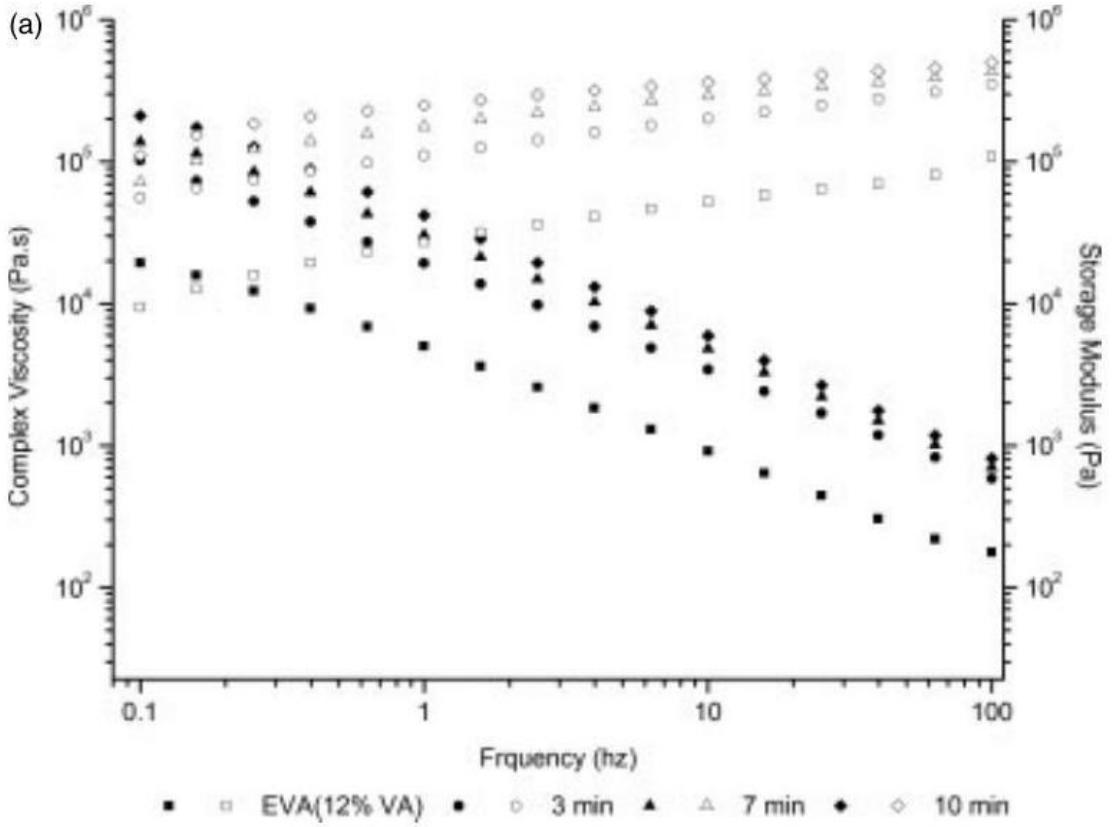
(a)
Complex Viscosity (Pa.s)
Storage Modulus (Pa)
Frquency (hz)
0.1
1
10
100
EVA(12% VA)
3 min
7 min
10 min

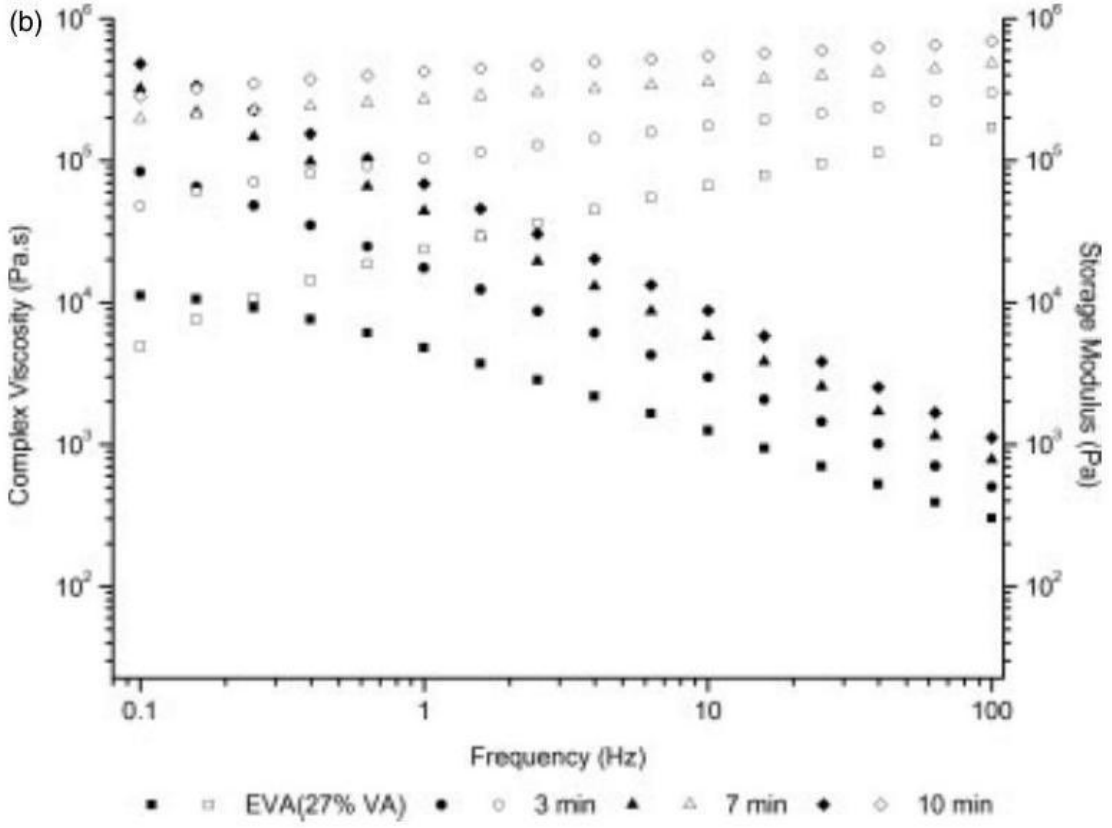
(b)
Complex Viscosity (Pa.s)
Storage Modulus (Pa)
Frequency (Hz)
0.1
1
10
100
EVA(27% VA)
3 min
7 min
10 min

Figure 2. Rheological behaviour of (a) HPNEVA12 and (b) HPNEVA27.

Table 1. Complex viscosity curve slopes for HPNEVA12 and HPNEVA27			
	3 min	7 min	10 min
HPNEVA12	-0.75	-0.78	-0.83
HPNEVA27	-0.76	-0.88	-0.89

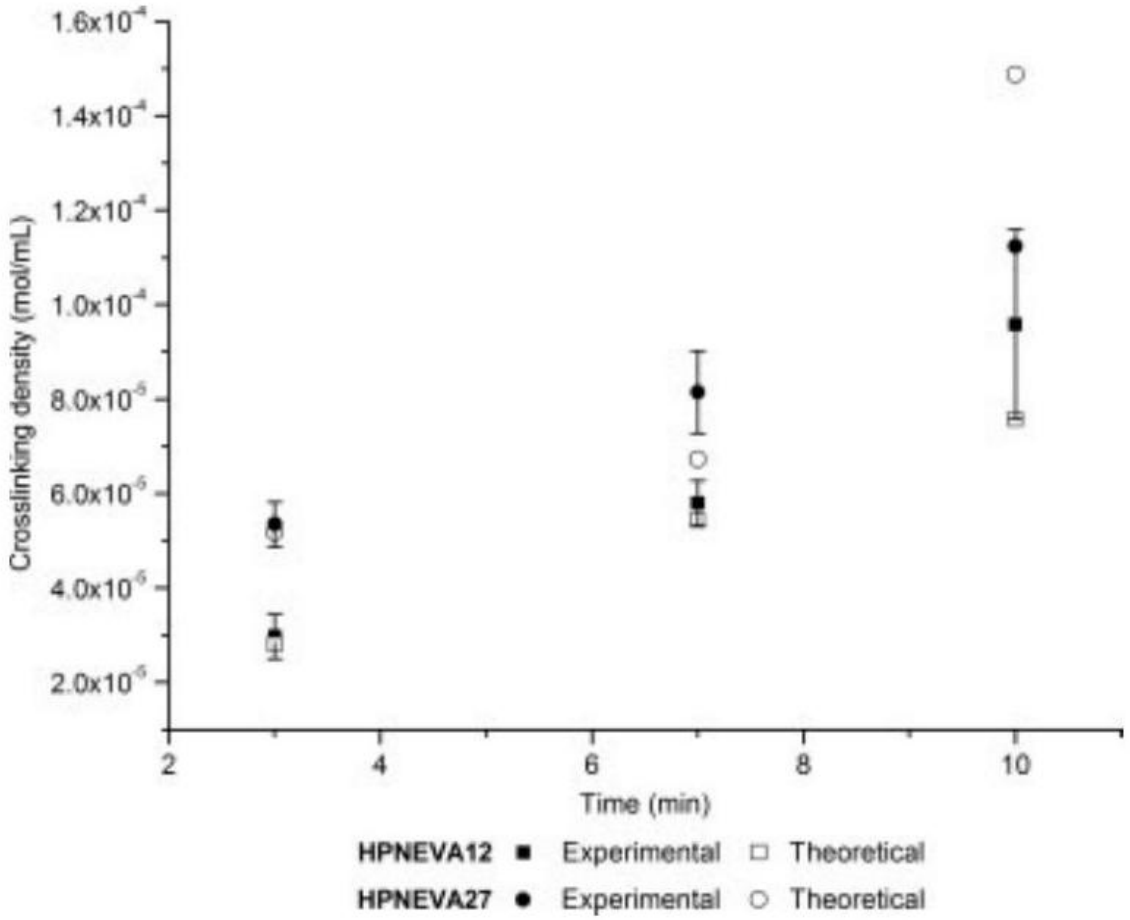

Figure 3. Crosslinking density evolution with reaction time for HPNEVA12 and HPNEVA27.

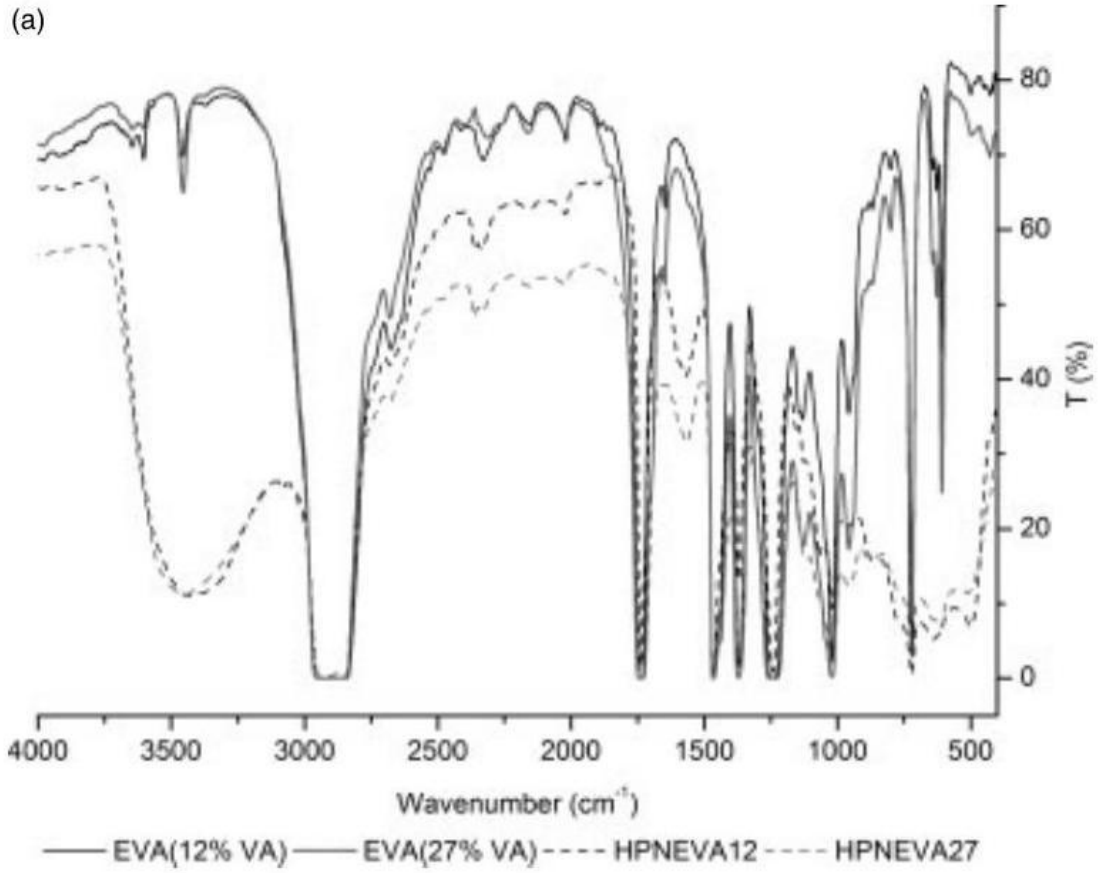
(a)
80
60
40
20
0
T (%)
4000
3500
3000
2500
2000
1500
1000
500
Wavenumber (cm-1)
EVA(12% VA)
EVA(27% VA)
HPNEVA12
HPNEVA27

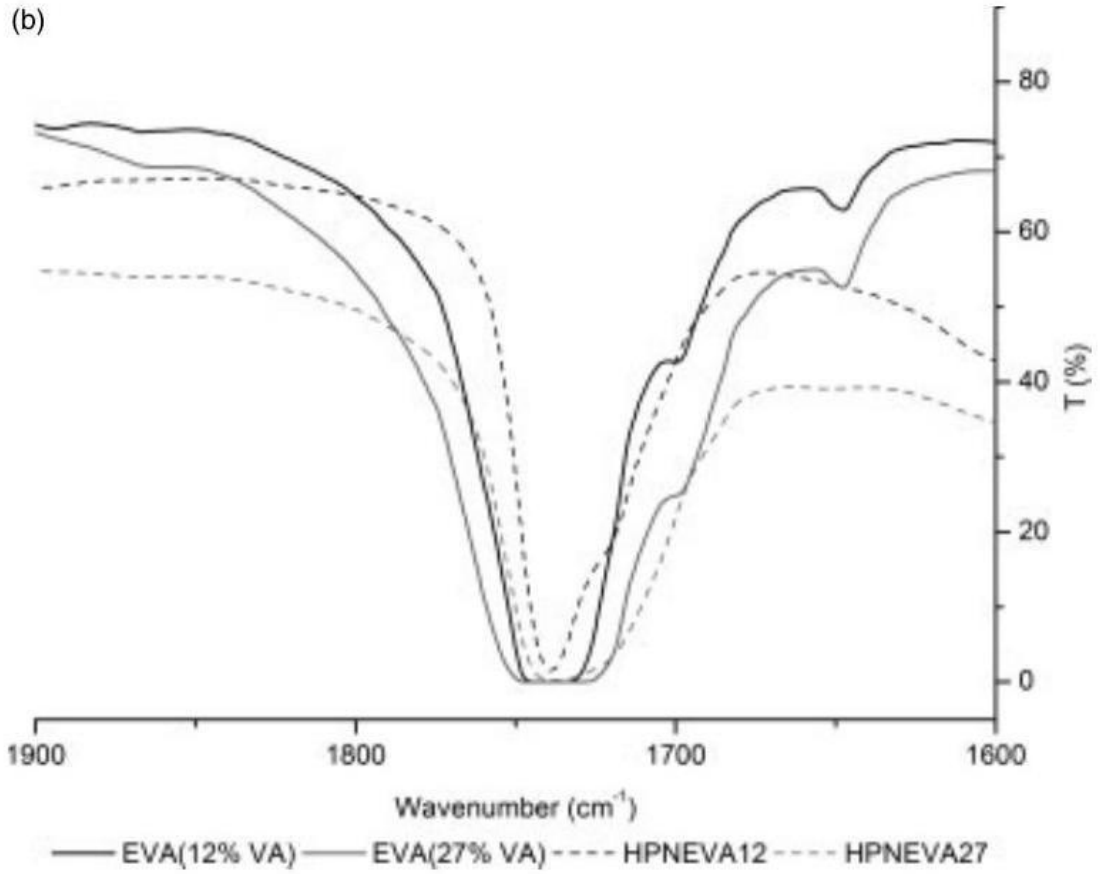
(b)
80
60
40
20
0
T (%)
1900
1800
1700
1600
Wavenumber (cm-1)
EVA(12% VA)
EVA(27% VA)
HPNEVA12
HPNEVA27

Figure 4. FTIR spectra: (a) EVA polymers and nanocomposites; (b) magnified view of the carbonyl band.

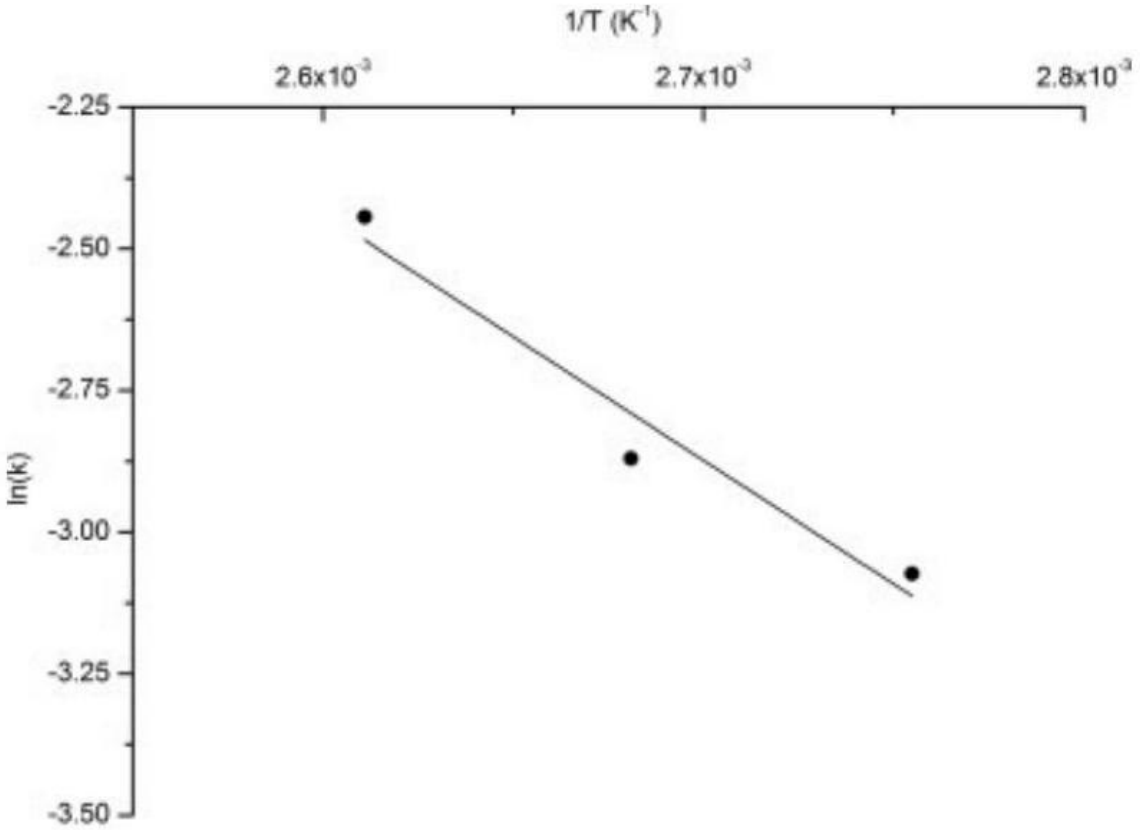

Figure 5. Arrhenius plot for the synthesis reaction of HPNEVA27. specimens 2 mm thick. The specimens were mounted in the vertical configuration and then were ignited from the bottom for 10 s.[13]

RESULTS AND DISCUSSION

The torque evolution with mixing time for HPNEVA12 and HPNEVA27 is shown in Fig. 1. The first peak is associated with

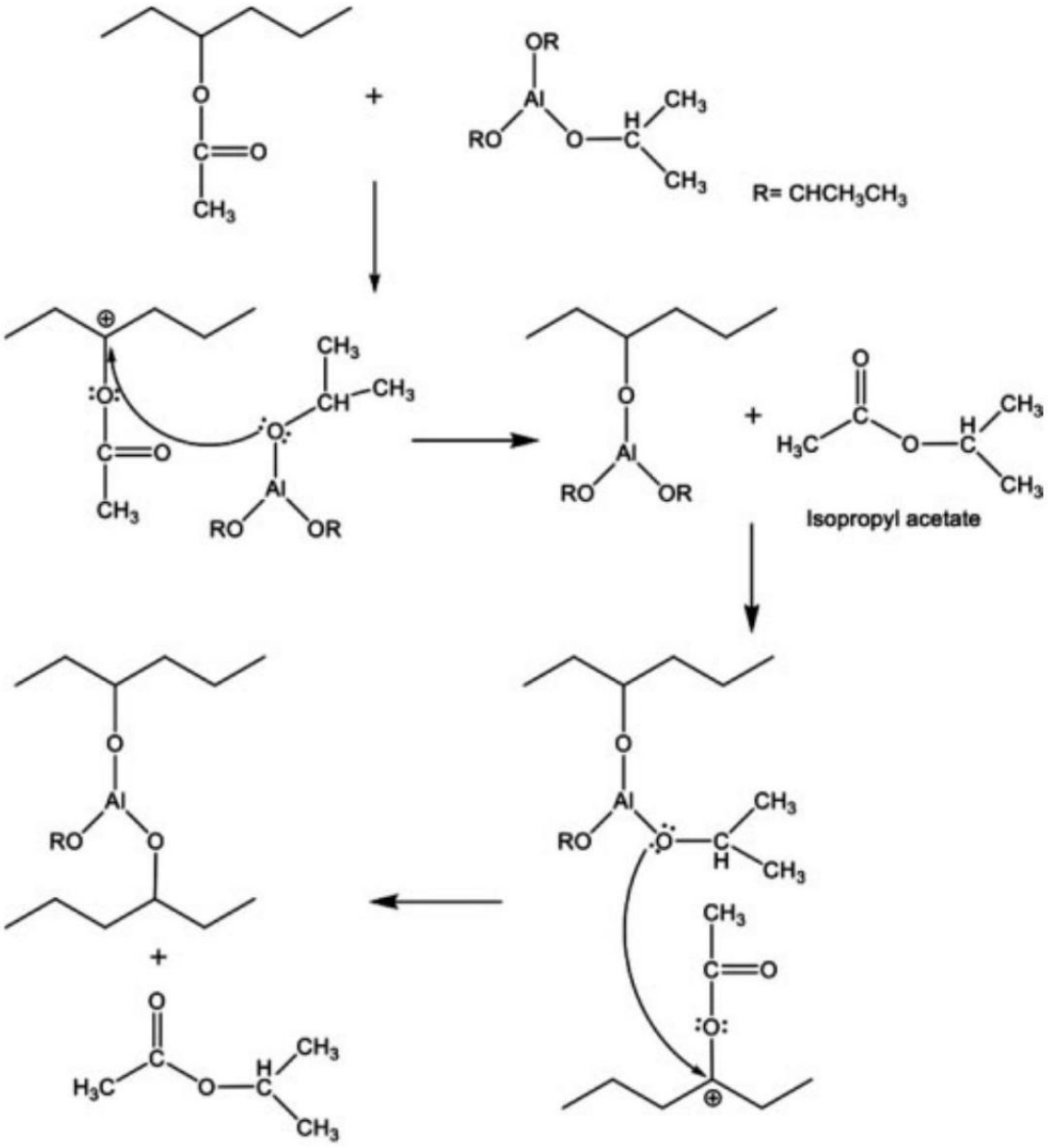

Figure 6. Reaction mechanism for the synthesis of EVA hybrids.

EVA melting followed by the addition of the aluminium precursor. The effect of the aluminium precursor on EVA chemical structure is clear - in both cases after the addition of the aluminium precursor the torque increased. This is due to the crosslinking reaction between VA groups and aluminium precursor. Since EVA27 has more VA groups, a more crosslinked structure is anticipated and consequently higher torque. However, EVA27 (71°C) has a lower melting temperature than EVA12 (96°C), which results in a decrease in viscosity and consequently a lower torque for HPNEVA27. Thus, the nanocomposite torque value was always under that for HPNEVA12. Moreover, as shown by Antunes et al., [14] a decrease of the torque values observed for HPNEVA27 at around 11 min can be attributed to network degradation. This phenomenon occurs for materials with very high crosslinking contents.

As shown in Fig. 2, for both EVAs the storage modulus and complex viscosity increase with reaction time as the crosslinking reaction takes place. Crosslinking affects the molecular motion and has a significant effect on rheological behaviour. [10] As the reaction takes place the material changes from liquid-like to solidlike material, where the storage modulus is independent of the frequency value. The nanocomposites prepared do not show a plateau at low frequencies and the complex viscosity has, in the limit, a slope of -1.[5] It is clear, for both HPNEVAs, that the evolution of the crosslinking structure is based on the curve slope values described in Table 1. Moreover, and despite the lower torque values, rheological measurements confirm that HPNEVA27 has a higher crosslinking level.

The storage modulus of the nanocomposites appeared to be constant over a very broad range of frequencies. From the theory of rubber elasticity, the equilibrium shear elasticity modulus (G_e) can be determined based on the slope of the tangent curve to G' at low frequencies. [10,14] Using G_e and the Flory-Rehner model coupled with the phantom network it is possible to predict the swelling results of an imperfect network:

$$v = \frac{G_e}{RT} \tag{5}$$

where v is the crosslinking density, R is the universal gas constant and T is the absolute temperature. G_e was obtained as the asymptotic value of G' at low frequency. The theoretical values of v determined using Eqn (5) and the experimental data measured by the swelling degree experiments are presented in Fig. 3.

Both EVAs show the same trend - the crosslinking density increases with time as a result of reaction evolution. Nevertheless, as expected HPNEVA27 exhibits higher crosslinking density values as a result of the greater amount of VA groups that react to form covalent bonds with aluminium particles. A different result was observed by Bounor-Legaré and co-workers: the crosslinking density decreased with time during the reaction between EVA and tetrapropoxysilane. [10] However, in their study the sol-gel reaction occurred during a post step treatment to promote the hydrolysiscondensation reaction. They explained the decrease as due to side reactions.

The theoretical crosslinking density values determined using Eqn (5) are in good agreement with the experimental results

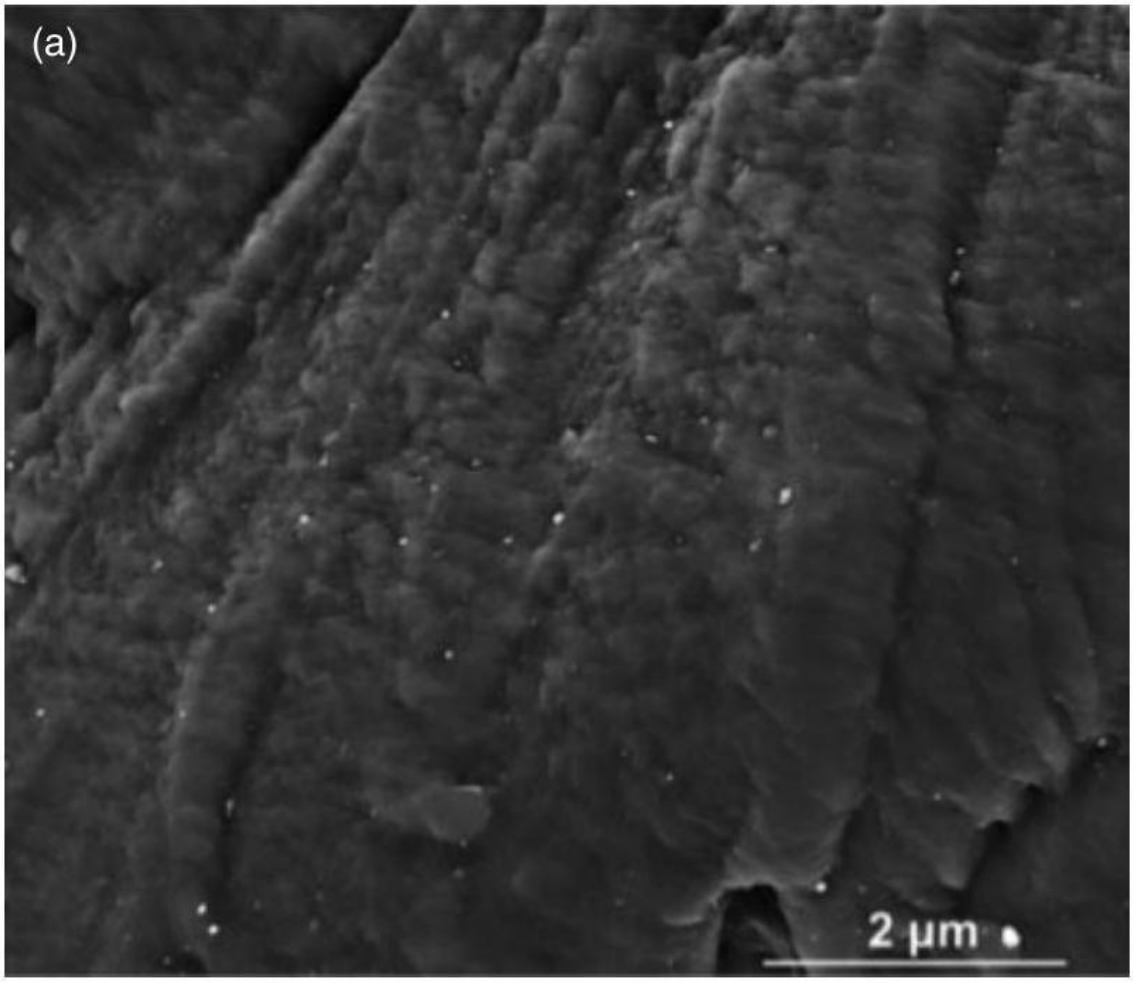
(a)
2 µm

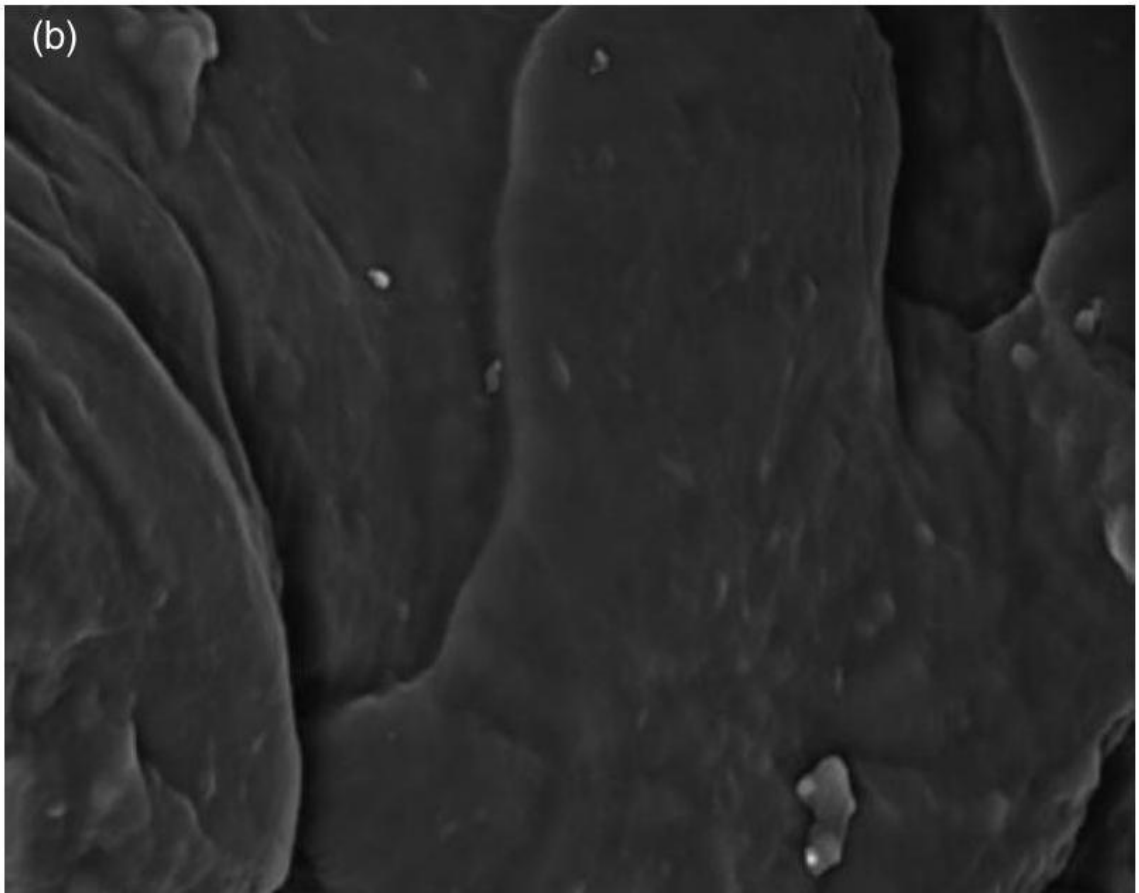
(b)

Figure 7. SEM micrographs of (a) the HPNEVA12 surface and (b) the HPNEVA27 surface. for reaction times of 3 and 7 min . A slight difference between theoretical and experimental values was observed for 10 min of reaction. This can be explained by the fact that at 10 min the G' values remained almost constant over a very broad range of frequencies; in this case G_e corresponds to the constant value of G'.[15]

FTIR analysis of the initial EVAs and nanocomposites are shown in Fig. 4. For both prepared hybrids the appearance of an OH band between 3000 and 3500 cm^{-1} confirms that the aluminium precursor suffered hydrolysis reactions with the respective bending mode band at 1627 cm^{-1} with medium intensity. Moreover, the Al-O stretching mode band between 400 and 1000 cm^{-1} can also be observed, which confirms that the sol-gel reaction has been successfully carried out. Differences can also be noticed in the peak of the $C = O$ stretching mode of the acetate group (Fig. 4(b)). After reaction, for both EVAs, the peak becomes less wide. This corroborates the reaction between the acetate groups and the precursor.

The reactivity was assessed by determination of the activation energy (E_a) involved in the synthesis of HPNEVA27. The Arrhenius plots obtained for HPNEVA27 are depicted in Fig. 5. A linear relationship was found corresponding to an E_a of

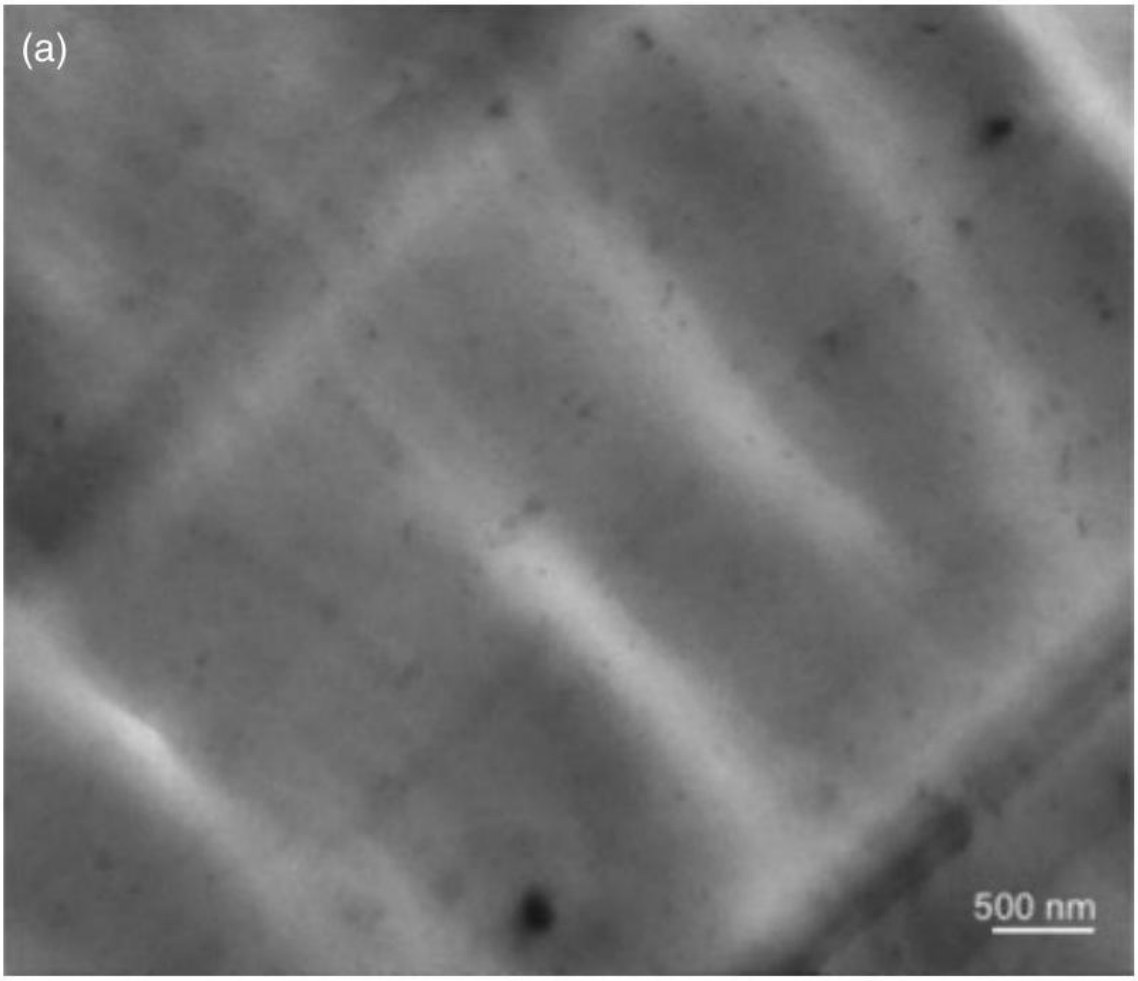
(a)
500 nm

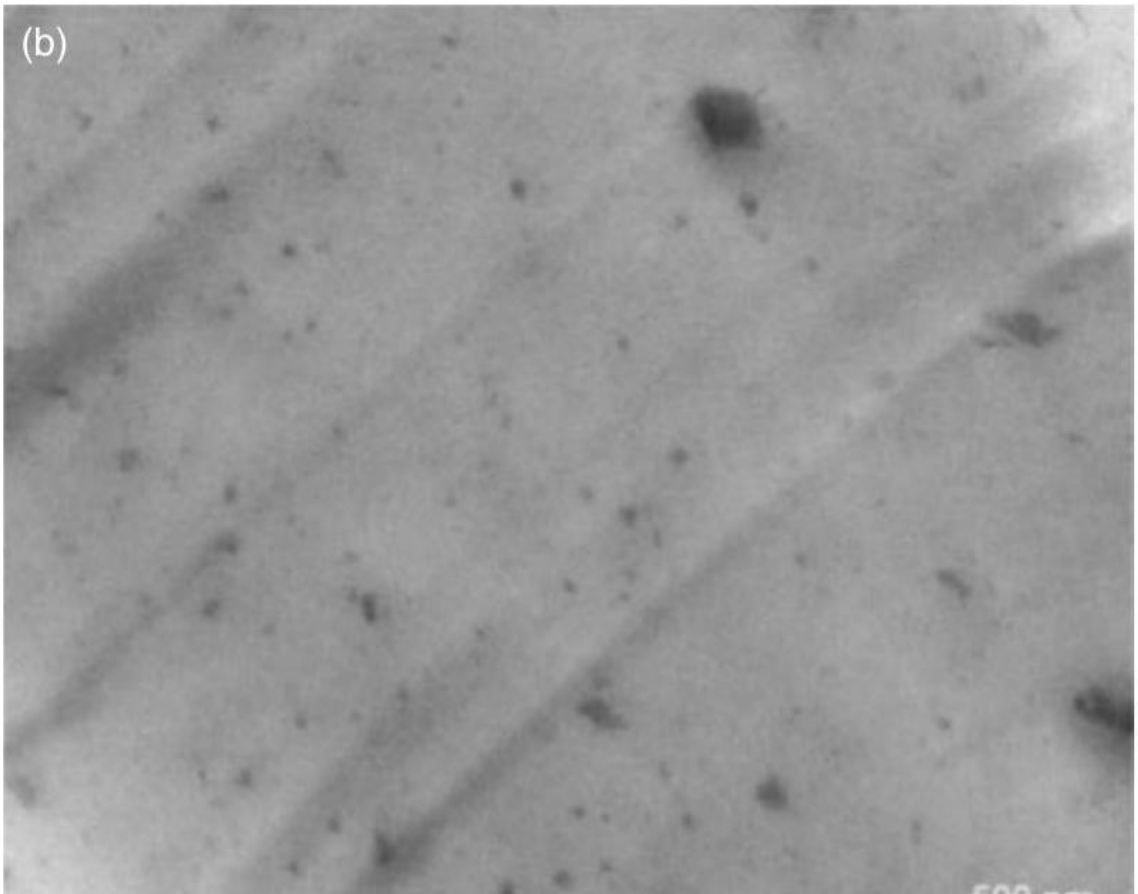
(b)

Figure 8. TEM micrographs of (a) HPNEVA12 and (b) HPNEVA27.

36.3 kJ mol^{-1}. Bounor-Legaré and co-workers obtained a similar E_a value (47 kJ mol^{-1}) for the synthesis of EVA (28% of VA) with tetraethoxysilane using dibutyltin oxide as catalyst. [10] The precursor $Al(Pr-i-O)_3$ was revealed to be very reactive, which can be explained by the linear organic chain ($-OC_3H_7$) with low stereochemical hindrance.

Taking into account the previous results a reaction mechanism can be proposed (Fig. 6). According to this chemical scheme the crosslinking structure was formed by nucleophilic attack of oxygen bonded to aluminium to the electropositive carbon of the acetate group. After the nucleophilic attack the acetate group leaves as isopropyl acetate. As $Al(Pr-i-O)_3$ is a trifunctional compound, a maximum of three bonds can take place leading to a crosslinking structure.

Backscattered electron microscopy was used to analyse the nanoparticle dispersion on EVA matrices. Backscattered electron micrographs presented in Fig. 7 show that HPNEVA12 and HPNEVA27 have homogeneous and smooth surfaces without particle agglomerates. In Fig. 7(a) the presence of small white shining dots can be observed well dispersed on the EVA surface. These dots were analysed by EDS as nanoparticles containing

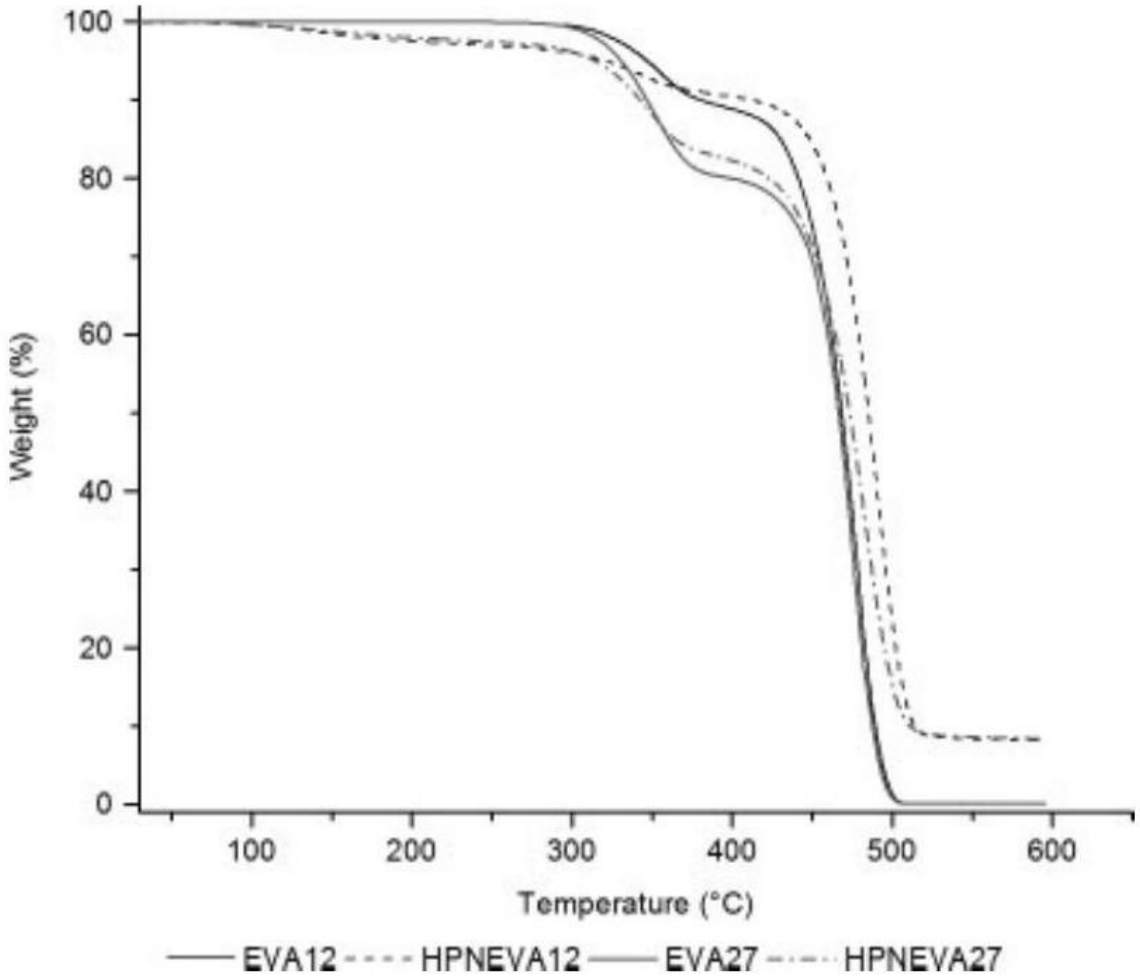

Figure 9. Evaluation of the thermal degradation of EVA matrices and hybrids. aluminium. Only a few white dots can be seen for HPNEVA27 (Fig. 7(b)), which might indicate a better dispersion and interaction between organic and inorganic components. As confirmed by rheology and crosslinking density results, the reaction was more extensive with this polymer. TEM micrographs (Fig. 8) confirm that, even though the nanoparticles are well dispersed in both EVA matrices, the dispersion seems better in EVA27. The average particle size is 130 and 120 nm for HPNEVA12 and HPNEVA27, respectively. The presence of aluminium at the material surface was analysed by EDS.

The thermal properties of EVA matrices and nanocomposites were tested under a nitrogen atmosphere and the data are presented in Fig. 9. The TGA results show that thermal degradation occurred in two distinct regions. The first around $300°C$ is assigned to the loss of acetic acid and the second around $400°C$ to the degradation of the resulting unsaturated material poly(ethylene-co-acetylene). [16] The HPNEVA12 and HPNEVA27 start to lose weight around $100°C$ due to evaporation of some residual reaction subproduct. During EVA hybrid synthesis, isopropyl acetate ($C_5H_7O_2$) is formed (Fig. 6), having a boiling point at $89°C$; this explains the first weight variation. Comparing the curves of EVA matrices and nanocomposites, it can be observed that the prepared materials show enhanced thermal stability at 50% weight loss. The crosslinking bonds between organic and inorganic components explain this behaviour. As expected, the residual weight obtained for both materials is similar.

Fire retardance tests were performed to study the effect of nanoparticles containing aluminium on the burning behaviour of HPNEVA12 and HPNEVA27. While specimens of EVA matrices burned very quickly (7 s), dripping at the same time, EVA nanocomposites exhibited higher resistance to flame propagation, increasing the combustion time (15 s), and the dripping effect was not observed. According to the UL Test Specifications, HPNEVA nanocomposites accomplish the $94\ V-0$ requirements.

CONCLUSION

This study shows that it is possible to prepare EVA nanocomposites with enhanced fire retardance by a method that can be used in the polymer processing industry. Since $Al(Pr-i-O)_3$ has a low activation energy, a post step treatment to promote the formation of metal nanoparticles is not required.

The rheology and crosslinking density values demonstrate that the metal is covalently bonded to the EVA structure forming a crosslinking structure. Morphological analysis corroborates that the nanoparticles are well dispersed. The reaction mechanism is proposed taking into account all the results obtained.

EVA nanocomposites achieve the requirements for $94\ V-0$ classification.

ACKNOWLEDGEMENTS

The authors acknowledge the Foundation for Science and Technology (FCT) Project SFRH/BD/39085/2007 for the financial support.

REFERENCES

1 Sanchez C, Shea K and Kitagawa S, Chem Soc Rev 40: 696-753 (2011).
2 Sadeghi M, Khanbabaei G, Dehaghani A, Sadeghi M, Aravand M, Akbarzade M, et al. J Membrane Sci 322: 423-428 (2008).
3 Bahloul W, Bounor-Lagaré V, David L and Cassagnau P, J Poly Sci Poly Phys 48: 1213-1222 (2010).
4 Cong H, Radosz M, Towler B and Shen Y, Separation Purif Techn 55: 281-291 (2008).
5 Oliveira M, Nogueira R and Machado A, React Funct Poly 72(10): 703-712 (2012).
6 Bounor-Legaré V, Angelloz C, Blanc P, Cassagnau P and Michel A, Polymer 45: 1485-1493 (2004).
7 Turova N, Turevskaya E, Kessler E and Yanovskaya M, The Chemistry of Metal Alkoxides. Kluwer Academic Publishers, Dordrecht (2002).
8 Brinker C and Scherer G, Sol-gel Science - The Physics And Chemistry OfSol-gel Processing. Academic Press, London, pp. 2-12 (1989).
9 Schottner G, Chem Mat 13: 3422-3435 (2001).
10 Bounor-Legaré V, Ferreira I, Verbois A, Cassagnau P and Michel A, Polymer 43: 6085-6092 (2002).
11 Zhang X, Guo J, Chen J, Wang G and Liu H, Polymer Degrad Stab 87: 411-418 (2005).
12 Shieh Y, Liau J and Chen T, J Appl Polym Sci 81: 186-196 (2001).
13 UL94. Test for Flammability of Plastic Materials for Parts in Devices and Applicances. Underwriters Laboratories, Northbrook, IL, 5th edn, pp. 24-26 (1996).
14 Antunes CF, Machado A and Duin M, Rubber Chem Technol J 82: 492-505 (2009).
15 Patel S, Malone S, Cohen C, Gilmor J and Colby H, Macromolecules 25: 5241-5251 (1982).
16 Costache M, Jiang D and Wilkie C, Polymer 46: 6947-6958 (2005).

M. Oliveira, IPC - Institute for Polymers and Composites/I3N, University of Minho, Campus de Azurém, 4800-058 Guimarães, Portugal. E-mail: moliveira@dep.uminho.pt

IPC - Institute for Polymers and Composites/I3N, University of Minho, Campus de Azurém, 4800-058, Guimarães, Portugal